

Severe encephalopathy associated to pyruvate dehydrogenase mutations and unbalanced coenzyme Q₁₀ content

Claudio Asencio^{1,2,7}, María A Rodríguez-Hernandez^{1,2,7}, Paz Briones^{2,3}, Julio Montoya^{2,4}, Ana Cortés^{1,2}, Sonia Emperador^{2,4}, Angela Gavilán^{1,2}, Eduardo Ruiz-Pesini^{2,4}, Dèlia Yubero^{2,3}, Raquel Montero^{2,5}, Mercedes Pineda^{2,5}, María M O'Callaghan^{2,5}, María Alcázar-Fabra^{1,2}, Leonardo Salvati⁶, Rafael Artuch^{2,5} and Plácido Navas^{*,1,2}

Coenzyme Q₁₀ (CoQ₁₀) deficiency is associated to a variety of clinical phenotypes including neuromuscular and nephrotic disorders. We report two unrelated boys presenting encephalopathy, ataxia, and lactic acidosis, who died with necrotic lesions in different areas of brain. Levels of CoQ₁₀ and complex II+III activity were increased in both skeletal muscle and fibroblasts, but it was a consequence of higher mitochondria mass measured as citrate synthase. In fibroblasts, oxygen consumption was also increased, whereas steady state ATP levels were decreased. Antioxidant enzymes such as NQO1 and MnSOD and mitochondrial marker VDAC were overexpressed. Mitochondria recycling markers Fis1 and mitofusin, and mtDNA regulatory Tfam were reduced. Exome sequencing showed mutations in PDHA1 in the first patient and in PDHB in the second. These genes encode subunits of pyruvate dehydrogenase complex (PDH) that could explain the compensatory increase of CoQ₁₀ and a defect of mitochondrial homeostasis. These two cases describe, for the first time, a mitochondrial disease caused by PDH defects associated with unbalanced of both CoQ₁₀ content and mitochondria homeostasis, which severely affects the brain. Both CoQ₁₀ and mitochondria homeostasis appears as new markers for PDH associated mitochondrial disorders.

European Journal of Human Genetics (2016) 24, 367–372; doi:10.1038/ejhg.2015.112; published online 27 May 2015

INTRODUCTION

CoQ₁₀ is a redox lipophilic molecule mainly located in inner mitochondria membrane that transfers electrons from complex I, and complex II to complex III in respiratory chain and participates in the superassembly of these complexes.¹ It has antioxidant properties, regulates both transition pore and uncoupling proteins, and it is an obligated substrate for both β -oxidation of fatty acids and pyrimidine nucleotide biosynthesis.² CoQ₁₀ deficiency impairs oxidative phosphorylation and causes clinically heterogeneous mitochondrial diseases,³ including an encephalomyopathy form with muscle disorders and myoglobinuria; an ataxic form with atrophic cerebellum; a severe infantile form with renal failure; an isolated myopathy, and nephrotic syndrome, have been so far described.⁴ Primary deficiencies are due to mutations of genes involved in its biosynthesis, a very complex pathway not completely known, whose regulation has started to be described.⁵ In mammals, CoQ levels are tissue specific and its concentration in mitochondria is very much balanced with electron chain complexes, contributing to prevent endogenous oxidative stress.⁶ Among tissues, CoQ content in brain is very stable and highly independent of environment.⁷ Furthermore, mutations of genes that are not part of respiratory chain also cause mitochondrial dysfunctions

and may induce an adaptive decrease of CoQ₁₀, named secondary deficiency, although the mechanisms are totally unknown.^{4,5}

In contrast to the already described cases of mitochondrial diseases showing CoQ₁₀ deficiency, we describe here two unrelated children that present a fatal neurological disorder, associated to genetic variants in *PDH* genes. The two cases presented high levels of both CoQ₁₀ and mitochondria in fibroblasts and skeletal muscle, with low efficient mitochondria that show defective homeostasis, and high levels of antioxidant enzymes.

SUBJECTS AND METHODS

Patient 1

This was a son from nonconsanguineous parents, with a negative family history. The parents had had two previous miscarriages. The boy presented the first clinical manifestations at 10 months old, showing hypertonus that lasted 1 week, with no other symptoms. One month later, during a viral process, he presented drowsiness, hypotonia, bilateral ptosis and ataxia, with a complete recovery after 15 days. At 18 months of age, after a febrile episode, he manifested ataxia, hypertonus and limitations of the upgaze; blood lactate values were markedly elevated. MRI evidenced basal ganglia lesions, in cerebellar pedunculi and bulbomedullar junction. In this occasion, after the resolution of the acute process, the patient manifested decreased strength in the

¹Centro Andaluz de Biología del Desarrollo, Universidad Pablo de Olavide-CSIC and CIBERER, Instituto de Salud Carlos III, Sevilla, Spain; ²Center for Biomedical Research on Rare Diseases (CIBERER), ISCIII, Madrid, Spain; ³Sección de Errores Congénitos del Metabolismo (IBC U737), Servicio de Bioquímica y Genética Molecular, Hospital Clínic de Barcelona, IDIBAPS and CSIC, Barcelona, Spain; ⁴Departamento de Bioquímica, Biología Molecular y Celular, Universidad de Zaragoza, Zaragoza, Spain; ⁵Clinical Chemistry, Departments of Pathology and Neurology, Hospital Sant Joan de Déu, Barcelona, Spain; ⁶Clinical Genetics Unit, Department of Woman and Child Health, University of Padova, and IRP Città della Speranza, Padova, Italy

*Correspondence: Dr P Navas, Centro Andaluz de Biología del Desarrollo, Universidad Pablo de Olavide-CSIC and CIBERER, Instituto de Salud Carlos III, Carretera de Utrera km 1, Sevilla 41013, Spain. Tel: +34 95 4349385; Fax: +34 95 4349376; E-mail: pnavas@upo.es

⁷These authors contributed equally to this work.

right part of the body. Under the suspicion of a mitochondrial disorder, muscle biopsy was performed. At age 2 years, he presented a new episode of acute ataxia with increased lactate values in both, blood and cerebrospinal fluid after which chronic ataxia persisted. Subsequently he presented repeated episodes, characterized by vomiting, worsening of ataxia, dysarthria, alteration of cranial nerves, loss of consciousness and hyperlactacidemia triggered by stress, physical exercise or febrile episodes. There was a progressive worsening of the general clinical condition during intercritical periods. Electromyography showed axonal neuropathy. The patient died at age 9 years and 5 months, after an acute febrile process, which triggered tonic-clonic seizures, loss of consciousness and marked brainstem dysfunction. MRI evidenced necrotic lesions in cortical, subcortical and supratentorial areas at basal ganglia, cerebellum, bulb, colliculi and mesencephalus.

Patient 2

He was the first son of nonconsanguineous parents, with a negative family history. Pregnancy and perinatal history were normal. The first clinical signs appeared at age 16 months with hypotonia, gait instability and vomiting during an upper respiratory tract infection, which resolved spontaneously without reliquates. At age 2 years and 6 months he was admitted to the hospital because of acute ataxia triggered by another upper respiratory tract infection. During infancy, he presented several other similar episodes during intercurrent diseases, characterized by acute ataxia, dysarthria, ptosis and acufens lasting from hours to several days. In the course of such episodes, both lactate and pyruvate values were increased in both blood and cerebrospinal fluid. Muscle biopsy was performed at age 3 years. Mild ataxia and mental disability became evident at age 11. Brain MRI showed T2 bilateral hyperintensities in lenticular nuclei, bulbar and right cerebellar hemisphere. Electroretinogram was normal. At age 16 years, during an infectious process, which evolved to sepsis, the patient developed severe lactic acidosis and brainstem dysfunction (with necrotic lesions in MRI), which rapidly lead to death.

Standard protocol approvals, registrations and patient consents
The Ethical Committee of Hospital Sant Joan de Déu approved the study.
Written informed consent was obtained from the parents to conduct the study.

Muscle and skin biopsies

Muscle biopsies were collected and stored, and skin biopsies were cultured following for both the standardized procedures previously reported.⁸ No CoQ₁₀ supplementation therapy was done prior to muscle or skin biopsies collection. All muscle biopsies were studied by standard histopathological procedures.

Fibroblasts culture

Control aged-matched human dermal fibroblasts (HDF) and patients skin fibroblasts (2 to 4 passes old) were cultured as described.⁹ Fibroblasts growth was determined in single plates for 144 h and counted each 24 h using a Neubaer chamber with an inverted microscope.

Mitochondrial biochemistry

CoQ₁₀ levels were determined and CoQ₁₀ biosynthesis rate was measured as the incorporation of the radiolabelled p-hydroxybenzoic acid ([¹⁴C]-pHB) as described.⁹ Activities of NADH:coenzyme Q₁ oxidoreductase (complex I), cytochrome C oxidoreductase (complex III), NADH:cytochrome C reductase (complex I+III), succinate:cytochrome C reductase (complex II+ III) and citrate synthase (CS) were determined in cell extracts using previously described spectrophotometric methods.¹⁰ Results are expressed as specific activity (μmol/min/mg protein; mean ± SD). Mitochondrial membrane potential (ΔΨ_m) and reactive oxygen species (ROS) generation were carried out as described.⁹ Proteins of fibroblasts homogenates were analyzed by the Lowry procedure.¹¹

ATP determination

ATP level was determined by bioluminescence method using commercial Molecular Probes' ATP Determination Kit (A22066). Assay is based on recombinant firefly luciferase requirement (and its substrate D-luciferin) for ATP in producing light emission maximum ~ 560 nm at pH 7.8 from the

reaction: luciferin+ATP+O₂ → (Mg²⁺+ luciferase) → oxyluciferin+AMP+pyrophosphate+CO₂+light. This assay is able to detect as little as 0.1 picomol of ATP. Standard curves were run with each experiment.

Molecular studies

Total DNA preparation was carried out following standard procedures. Exomes were tested against the Single Nucleotide Polymorphism (dbSNP) and the 1000 genome project databases (1000 g) and the ESP 5400 data release of the NHLBI GO Exome Sequencing Project (ESP5400). 'Sorting tolerant from intolerant' (sift) and 'polymorphism phenotyping' (polyphen) algorithms were used to predict the consequences of the variations. Candidate variants were confirmed by standard sequencing procedure of genomic and/or cDNA fragments. RNA was extracted with easy-BLUE Total RNA Extraction kit (iNtRON Biotechnology) according to manufacturer's instructions. One microgram of total RNA was used to obtain cDNA of *PDH* genes with the iScript cDNA Sintesis Kit (Bio-Rad) following manufacturer's instructions. Reference sequences NG_016781.1 and NM_000284.3 for *PDH1* and NG_016860.1 and NM_000925.3 for *PDH2* were used in this study. Variants and phenotypes described herein are accessible in the gene variant database at <http://databases.lovd.nl/shared/screenings/0000032781> (individual ID 00032713) and <http://databases.lovd.nl/shared/screenings/0000032784> (individual ID 00032716) for *PDH1* and *PDH2* respectively. Exons in *PDH* gene are numbered as in NG_016860.1. Primers 5'-0ATGAGGAAGATGCTCGCC-3' and 5'-TTAACTGACTGACTTAACTTGATCC-3' were used to PCR amplify and validate variant c.832G4A in *PDH1* cDNA from patient 1. Primers 5'-CCTGAGGGCATGTCTGTGA-3' and 5'-CAGGCTGGACAACAGAGTGA-3' were used to confirm variant c.301A4G in *PDH2* gene from genomic DNA of patient 2. Primers 5'-GGTCACCGCCTACTGTCAAT-3' and 5'-GCAGGAGAGAGGAAGATGA-3' were used to confirm variant c.42+1G4A in *PDH2* gene from genomic DNA of patient 2. To investigate the effect of the c.42+1G4A variant, a 521 bp cDNA fragment from *PDH2* gene in patient 2 was amplified with primers 5'-CTGGCTTGGTGCAGGAGAC-3' and 5'-CCAGGGACTGACCACCTTTA-3' (primers F1 and R1 in Figure 2, respectively). Bands were purified and cloned in plasmid pYES 2.1 TOPO (Invitrogen, Madrid, Spain). Alternative splicing caused by c.42+1G4A variant was confirmed by PCR amplification of cloned fragments with primers F1, R1 and R2 (5'-GCAGGGAGAGAGGAAGATGA-3') and later sequencing. See Figure 2e for a schematic representation of the strategy followed to prove alternative splicing of intron 1 due to variant c.42+1G4A in *PDH2* from patient 2. Mitochondrial DNA from both patients was sequenced by standard procedure.

Immunoblotting

Western blotting was performed using standard methods. After protein transfer, membrane was incubated with primary antibodies against NQO1 (sc-16464, Santa Cruz Biotechnology, Heidelberg, Germany), MnSOD (574596, Calbiochem, Barcelona, Spain), TFAM (sc-23588, Santa Cruz Biotechnology), PGC-1α (516557, Calbiochem), VDAC/Porin (AV35122, Sigma, Madrid, Spain), Mitofusin (ab57602, Abcam, Madrid, Spain) and Fis1 (ALX-210-1037-0100, Enzo Life Sciences, Inc., Madrid, Spain). Corresponding rabbit anti-goat (SC-2768, Santa Cruz Biotechnology), goat anti-rabbit (401353, Calbiochem), goat anti-mouse (401253, Calbiochem) or rabbit anti-sheep (402100, Calbiochem) secondary antibodies coupled to horseradish peroxidase were later applied. Specific protein complexes were identified using HRP substrate.

Statistical analysis

All results are expressed as mean ± SD of three independent experiments. The measurements were statistically analyzed using Student t-test for comparing two groups. The level of significance was set at *P* ≤ 0.05.

RESULTS

Histology of muscle of P1 showed few muscle fibers with the presence of morphologically abnormal mitochondria with no other histopathological signs. Optic microscopy showed abnormal fibers with subsarcolemmal deposits suggestive of a mitochondrial disorder in

Table 1 Mitochondria properties of patient's samples

Activities	Skeletal muscle			Skin fibroblasts		
	Control	P1	P2	Control	P1	P2
CoQ ₁₀ μ mol/mg prot	0.11–0.48	0.59	0.84 ^a	100 \pm 45	105.7 \pm 36 ^a	114.2 \pm 40 ^a
CoQ ₁₀ μ mol/CS units	2.6–8.4	18.3	26.1 ^a	1.42 \pm 0.6	0.69 \pm 0.1	1.11 \pm 0.6
[¹⁴ C]-CoQ ₁₀ % vs control	—	—	—	100 \pm 11	186 \pm 31 ^b	207 \pm 29 ^b
[¹⁴ C]-CoQ ₁₀ /CS units % vs control	—	—	—	118.6 \pm 26.4	130.1 \pm 24.2	306.9 \pm 22.5 ^b
Citrate synthase (CS) nmol/min/mg prot	71–200	85	96	351 \pm 2	676 \pm 14 ^b	365 \pm 37
Complex I+III nmol/min/mg prot	12–56	43	49	299 \pm 20	404 \pm 41 ^b	289 \pm 21
Complex I+III Act/CS units	107–560	506	250	274.5 \pm 12	314.3 \pm 19	253.2 \pm 13
Complex II+III nmol/min/mg prot	7–24	25	34 ^a	2.9 \pm 0.1	3.8 \pm 0.3 ^a	4.9 \pm 0.7 ^b
Complex II+III Act/CS units	60–149	224	122	3.37 \pm 1.17	1.92 \pm 0.14	3.22 \pm 1.94
Complex IV nmol/min/mg prot	—	—	—	75.4 \pm 7.4	58.8 \pm 9.6	63.5 \pm 14.7
Complex IV Act/CS units	—	—	—	68.6 \pm 16.4	68.1 \pm 18.1	75.3 \pm 17.0
Membrane potential $\Delta\psi$ m (a.u.)	—	—	—	22.8 \pm 1.1	26.5 \pm 2.0 ^a	27.9 \pm 0.3 ^a
Oxygen consumption % vs control	—	—	—	100	222.34 ^b	127.65 ^a

^aSignificant versus control $P \leq 0.05$.^bSignificant versus control $P \leq 0.005$.

P2 muscle. Muscle CoQ₁₀ content was slightly increased in P1 (0.59 μ mol/mg prot; controls: 0.11–0.48) and more significantly in P2 (0.84 μ mol/mg of protein), which were also higher when referred to citrate synthase (Table 1). CoQ₁₀ content and biosynthetic rates were significantly increased in fibroblasts of both patients that corresponded to the increase of mitochondrial mass (Table 1). Complex I+III activity was in the upper level of reference values in muscle of both patients, and was significantly higher in fibroblast from P1. Complex II+III activity was also at the upper reference value in P1 muscle and was significantly higher in both P2 muscle and fibroblasts of both patients (Table 1). Both activities corresponded to higher mitochondria in these fibroblasts as indicated when referred to citrate synthase. Complex IV activity was unaffected in patient's fibroblasts (Table 1). These results correlated with a significant increase of both mitochondrial membrane potential and oxygen consumption in fibroblasts of both patients (Table 1). Lactate accumulation in media after 48 h growth was higher in P1 fibroblasts (82.9 \pm 4.8 a.u./cells number, $P \leq 0.05$) and P2 fibroblasts (75.6 \pm 7.0 a.u./cells number, $P \leq 0.05$) compared with control cells (45.2 \pm 6.6 a.u./cells number). The unbalanced mitochondria showed a low efficiency when ATP levels were referred to citrate synthase in these fibroblasts (Figure 1a), and patient's fibroblasts also showed a higher growth rate than control (Figure 1b). The patients did not present deletions and depletions of the mtDNA and sequencing of the whole mtDNA did not show any pathological mutation. However, mtDNA function must be affected in both patients' fibroblasts owing to the significant decrease of Tfam but not mitochondria biogenesis owing to the unchanged expression of PGC1 α (Figure 1c). The increased level of VDAC/porine determined by immunoblotting in both fibroblasts confirmed the higher mitochondria mass determined by citrate synthase. Likewise, mitochondrial recycling was also affected as Fis1 and mitofusin were decreased in these fibroblasts (Figure 1c). In order to understand the physiology of these cells that are representative of somatic cells from patients, we analyzed reactive oxygen species (ROS) generation that did not show differences with control but antioxidant enzymes NQO1 and MnSOD were clearly increased explaining the low ROS concentration (Figure 1c).

In order to approach for the molecular origin of the disease we developed the sequence of the whole exome of both patients (the complete sequence information is available upon request).

Variants were filtered following criteria of a minor allele frequency lower than 0.5% in the 1000 genome database and expected protein damage according to SIFT and Polyphen algorithms (see Subjects and Methods). In this way, variants compatible with the clinical symptoms of both patients were found in genes encoding for subunits of the pyruvate dehydrogenase complex. Patient 1 presented a c.832G4A substitution at the coding region of the *PDHA1* gene, leading to a p (G278R) change at the E1 α subunit of the PDH complex (Figure 2a). The p(G278R) change at *PDHA1* has been previously described to affect the stability of the PDH complex resulting in a reduction by 60% of the total PDH activity in fibroblasts from patients.¹² The c.832G4A variant in *PDHA1* was a *de novo* mutation as it was absent in all, the parents and a healthy brother of patient 1. Patient 2 presented two variants in compound heterozygosis at the *PDHB* gene, which encodes the E1 β subunit of the PDH complex. The c.301A4G variant, maternally inherited, led to a methionine to valine substitution at position 101 (Figure 2b). M101 is a highly conserved amino acid and p.M101V and p.M101T substitutions have been observed in other patients with reduced PDH activity in both, fibroblasts and skeletal muscle.¹³ The second variant, paternally inherited, is a novel c.42+1G4A substitution, affecting the first nucleotide of the first intron of the *PDHB* gene (Figure 2c). PCR amplification of a region comprising the first 500 bp of the *PDHB* cDNA resulted in double bands in patient 2. The detection of a weak upper band suggested an aberrant mRNA maturation compatible with the lack of splicing of the first intron and the consequent degradation of the messenger (Figure 2d). Both bands were cloned in pYES 2.1 TOPO plasmid and a second PCR was done using a forward primer aligned to the plasmid backbone and a reverse primer aligned to the end of first intron (Figure 2e). Amplification was only observed with the sample containing the cloned upper band (Figure 2f), supporting that the observed double band corresponded to alternatively spliced molecules of *PDHB* mRNA. The reverse primer used in this experiment aligned three nucleotides before the second exon (Figure 2e). This suggests that the c.42+1G4A variant does not promote the appearance of an alternative splicing site, but a complete absence of maturation of the first intron. This hypothesis was finally confirmed by direct sequencing of both cloned cDNA fragments, finding that the c.42+1G4A variant avoids the maturation of the first intron, resulting in a premature stop codon at the second exon (data not shown) and the consequent

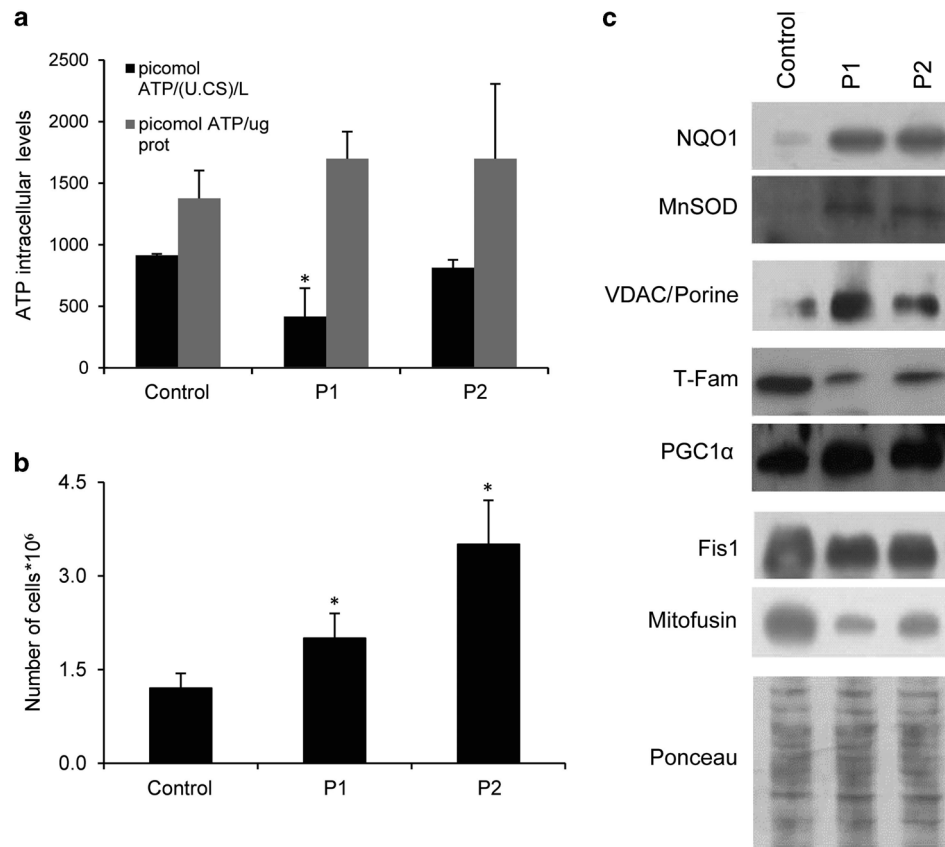


Figure 1 Properties of skin fibroblasts of P1 and P2. (a). ATP content in control and patients fibroblasts. Results are expressed as mean \pm SD of three independent experiments. * $P < 0.05$ between control and patients fibroblasts. (b). Fibroblasts proliferation at 144 h from seeding. Both control and patients' fibroblasts were seeded at a initial concentration of 1.75×10^5 cells per well. Results are expressed as mean \pm SD of three independent experiments. * $P < 0.05$ between control and patients fibroblasts. (c). Immunolocalization of antioxidant enzymes NADH quinone oxidoreductase (NQO1) and Manganese Superoxide dismutase (MnSOD); Mitochondrial protein VDAC/Porine; Mitochondrial transcription activator TFam and PGC1 α ; Pro-fission protein FIS1 and Pro-fusion protein Mitofusin. Ponceau staining reflects equal protein loading.

degradation of the affected mRNA molecules. Importantly, the c.42 +1G4A variant was also found in a healthy brother of patient 2 whereas the variant c.301A4G was absent. This result, together with the single variants found in the parents of patient 2 confirms that

PDHB deficiencies are associated to homozygous or compound heterozygous mutations.

DISCUSSION

The content of CoQ₁₀ in mitochondria is very much balanced with respiratory chain complexes contributing to their superassembly,¹ which contributes to the efficiency of oxidative phosphorylation and limiting ROS production.⁶ Also, CoQ levels in brain are remarkably stable in mammals and are independent from environment.⁷ This is the base of understanding that a defective biosynthesis of CoQ₁₀ by mutations in any COQ genes, and secondary deficiencies by defects of respiratory chain complexes functions such as mtDNA depletions¹⁴ or proteins involved in mitochondrial homeostasis cause mitochondrial diseases mainly with neuromuscular phenotype.⁵ The two patients presented here showed a similar phenotype to those described in encephalomyopathy, mainly ataxia, associated to primary or secondary CoQ₁₀ deficiency but in these cases CoQ₁₀ levels were elevated in both muscle and fibroblasts, corresponding to the increase of mitochondrial mass, showing mitochondrial dysfunction with low efficiency on ATP biosynthesis. A similar condition of defective respiration in the

presence of high content of CoQ has been described in COQ10 null mutant yeast strain,¹⁵ indicating that CoQ is one major component in respiratory chain but requires proteins for its electron carrier transport to properly prevent defective electrons leaking for ROS production. Elevated levels of ROS have been observed in PDH-deficient fibroblasts, probably produced at the Q site in complex III. We were unable to detect ROS production in fibroblasts of patients, however the over-expression of antioxidant enzymes MnSOD and NQO1, which is also a superoxide scavenger,¹⁷ demonstrates that electron leaking is indeed happening. Furthermore, NQO1 catalyzes NAD(P)H oxidation by reducing CoQ₁₀¹⁸ that would compensate the redox balance of the high CoQ₁₀ content. Also, the microscopy discovery of abnormal mitochondria correlates with the decrease of mitochondria recycling enzymes demonstrating the accumulation of low efficient mitochondria. The unbalanced mitochondria were also confirmed by the decrease of Tfam, which regulates expression and maintenance of mtDNA.¹⁹

The variants detected in PDH complex after exome sequencing would explain the clinical phenotype that has been previously described in patients with mutations in genes of this complex.¹³ In these cases, the rise of mitochondria and the corresponding CoQ₁₀ concentration would try to compensate the lack of acetyl-CoA and also to contribute to NQO1 activity to prevent oxidative damage. These results indicate the importance of the balanced requirement for CoQ₁₀ and electron chain complexes, and also promote that early

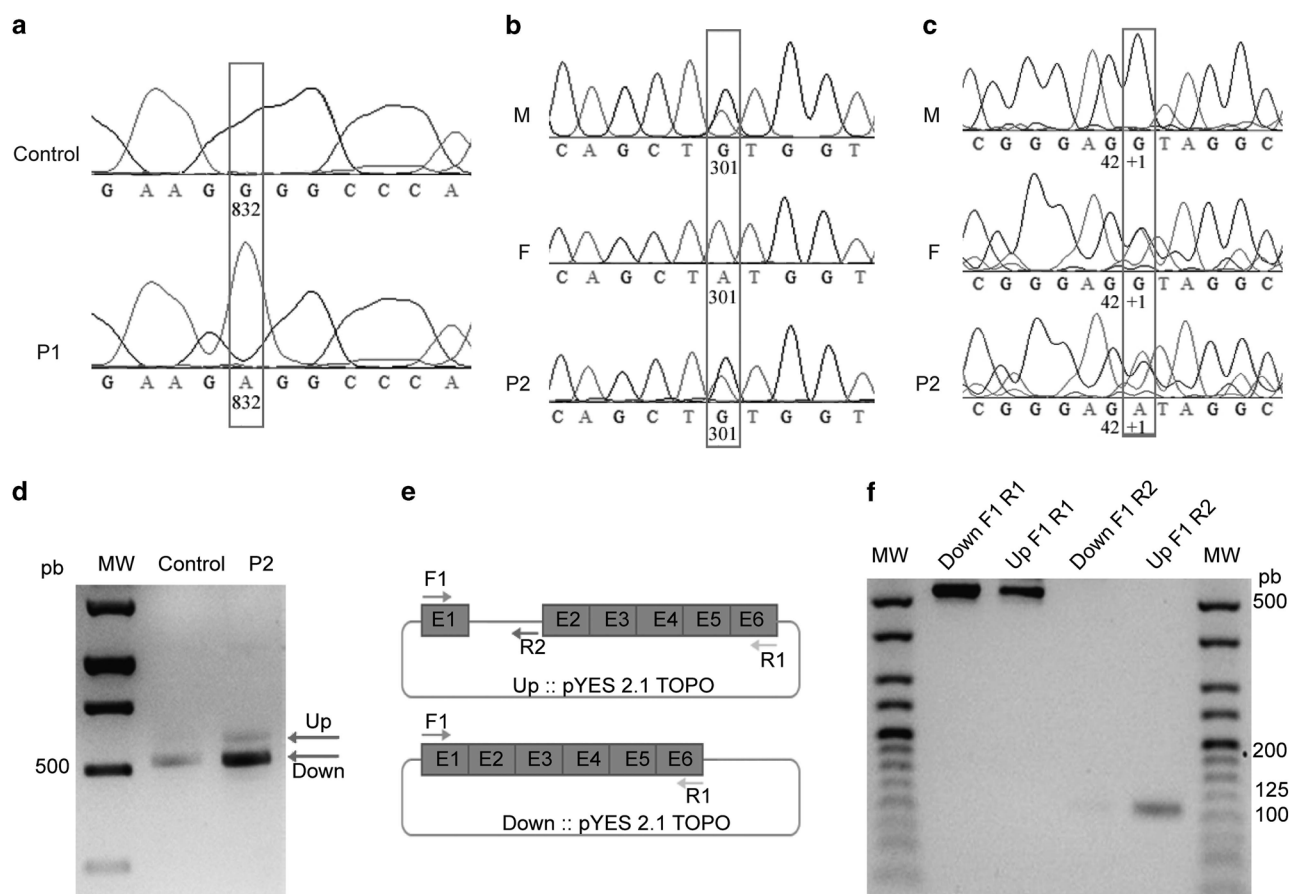


Figure 2 Mutations in genes encoding for PDH complex subunits. (a). Sequencing of c.832G4A mutation (red square) in PDHA1 cDNA from patient 1. (b) Sequencing of maternally inherited c.301A4G mutation (red square) in PDHB cDNA, leading to p.M101V substitution. (c) Sequencing of paternally inherited substitution c.42+1G4A (red square) in genomic DNA, leading to altered splicing of intron of PDHB gene in patient 2. (d) PCR amplification of a 500 pb cDNA fragment of PDHB from patient 2 and control. Arrow indicates the alternatively matured mRNA including the unspliced first intron. (e) Schematic representation of up and down fragments cloned in pYES 2.1 TOPO vector. Exons are represented as boxes, unspliced intron in UP fragment as a blue line and backbone of pYES 2.1 TOPO vector in orange. F1, R1 and R2 primers were used to prove the alternative splicing of PDHB gene in patient 2. (f) PCR amplification of Up and Down cloned cDNA fragments observed in patient 2 in figure (d). M, F and P2 in 2B and 2C panels correspond to mother, father and patient 2, respectively. The full colour version of this figure is available at *European Journal of Human Genetics* online.

diagnosis of CoQ₁₀ content and citrate synthase are required to predict new clinical phenotypes of mitochondrial diseases.

CONFLICT OF INTEREST

The authors declare no conflict of interest.

ACKNOWLEDGEMENTS

We thank the Bioinformatics Platform for Rare Diseases (CIBERER BIER), Valencia, Spain, for their help in the analysis of the exome sequencing data. This research was funded by grants PI14/00028 (RA), PI10-00662 (JM), and PI14/01962 (PN) from the Spanish Ministry of Health (Fondo de Investigación Sanitaria, Instituto de Salud Carlos III). LS was funded by Telethon Italy (GGP13222), the University of Padova (CPDA123573/12), and Fondazione CARIPARO (to LS). CA was funded by grant APP2D11086 from the University Pablo de Olavide (Plan Propio de Investigación).

- Bentinger M, Tekle M, Dallner G: Coenzyme Q-biosynthesis and functions. *Biochem Biophys Res Commun* 2010; 396: 74–79.
- Emmanuele V, López LC, López L *et al*: Heterogeneity of coenzyme Q10 deficiency: patient study and literature review. *Arch Neurol* 2012; 69: 978–983.
- Laredj LN, Licitra F, Puccio HM: The molecular genetics of coenzyme Q biosynthesis in health and disease. *Biochimie* 2014; 100: 78–87.
- Doimo M, Desbats MA, Cerqua C, Cassina M, Trevisson E, Salvati L: Genetics of coenzyme Q10 deficiency. *Mol Syndromol* 2014; 5: 156–162.
- Genova ML, Lenaz G: Functional role of mitochondrial respiratory supercomplexes. *Biochim Biophys Acta* 2014; 1837: 427–443.
- Parrado-Fernández C, López-Lluch G, Rodríguez-Bies E *et al*: Calorie restriction modifies ubiquinone and COQ transcript levels in mouse tissues. *Free Radic Biol Med* 2011; 50: 1728–1736.
- Montero R, Sánchez-Alcázar JA, Briones P *et al*: Analysis of coenzyme Q10 in muscle and fibroblasts for the diagnosis of CoQ10 deficiency syndromes. *Clin Biochem* 2008; 41: 697–700.
- López-Martín JM, Salvati L, Trevisson E *et al*: Missense mutation of the COQ2 gene causes defects of bioenergetics and de novo pyrimidine synthesis. *Hum Mol Genet* 2007; 16: 1091–1097.
- Spinazzi M, Casarin A, Pertegato V, Salvati L, Angelini C: Assessment of mitochondrial respiratory chain enzymatic activities on tissues and cultured cells. *Nat Protoc* 2012; 7: 1235–1246.
- Lowry OH, Rosebrough NJ, Farr AL, Randall RJ: Protein measurement with the Folin phenol reagent. *J Biol Chem* 1951; 193: 265–275.
- Imbard A, Boutron A, Vequaud C *et al*: Molecular characterization of 82 patients with pyruvate dehydrogenase complex deficiency. Structural implications of novel amino acid substitutions in E1 protein. *Mol Genet Metab* 2011; 104: 507–516.

1 Lapuente-Brun E, Moreno-Loshuertos R, Acín-Pérez R *et al*: Supercomplex assembly determines electron flux in the mitochondrial electron transport chain. *Science* 2013; 340: 1567–1570.

- 13 Quintana E, Mayr JA, García Silva MT *et al*: PDH E1 β deficiency with novel mutations in two patients with Leigh syndrome. *J Inherit Metab Dis* 2009; 32(Suppl 1): S339–S343.
- 14 Montero R, Grazina M, López-Gallardo E *et al*: Coenzyme Q₁₀ deficiency in mitochondrial DNA depletion syndromes. *Mitochondrion* 2013; 13: 337–341.
- 15 Barros MH, Johnson A, Gin P, Marbois BN, Clarke CF, Tzagoloff A: The *Saccharomyces cerevisiae* COQ10 gene encodes a START domain protein required for function of coenzyme Q in respiration. *J Biol Chem* 2005; 280: 42627–42635.
- 16 Glushakova LG, Judge S, Cruz A, Pourang D, Mathews CE, Stacpoole PW: Increased superoxide accumulation in pyruvate dehydrogenase complex deficient fibroblasts. *Mol Genet Metab* 2011; 104: 255–260.
- 17 Siegel D, Gustafson DL, Dehn DL *et al*: NAD(P)H:quinone oxidoreductase 1: role as a superoxide scavenger. *Mol Pharmacol* 2004; 65: 1238–1247.
- 18 Winski SL, Koutalos Y, Bentley DL, Ross D: Subcellular Localization of NAD(P)H:quinone Oxidoreductase 1 in Human Cancer Cells. *Cancer Res* 2002; 62: 1420–1424.
- 19 Gomes AP, Price NL, Ling AJY *et al*: Declining NAD(+) induces a pseudohypoxic state disrupting nuclear-mitochondrial communication during aging. *Cell* 2013; 155: 1624–1638.